

Chapter 2

The Physics of Plasticity

Section 2.1 Phenomenology of Plastic Deformation

The adjective “plastic” comes from the classical Greek verb *πλάσσειν*, meaning “to shape”; it thus describes materials, such as ductile metals, clay, or putty, which have the property that bodies made from them can have their shape easily changed by the application of appropriately directed forces, and retain their new shape upon removal of such forces. The shaping forces must, of course, be of sufficient intensity — otherwise a mere breath could deform the object — but often such intensity is quite easy to attain, and for the object to have a useful value it may need to be hardened, for example through exposure to air or the application of heat, as is done with ceramics and thermosetting polymers. Other materials — above all metals — are quite hard at ordinary temperatures and may need to be softened by heating in order to be worked.

It is generally observed that the considerable deformations which occur in the plastic shaping process are often accompanied by very slight, if any, volume changes. Consequently plastic deformation is primarily a *distortion*, and of the stresses produced in the interior of the object by the shaping forces applied to the surface, it is their deviators that do most of the work. A direct test of the plasticity of the material could thus be provided by producing a state of simple shearing deformation in a specimen through the application of forces that result in a state of shear stress. In a soft, semi-fluid material such as clay, or soil in general, this may be accomplished by means of a direct shear test such as the shear-box test, which is discussed in Section 2.3. In hard solids such as metals, the only experiment in which uniform simple shear is produced is the twisting of a thin-walled tube, and this is not always a simple experiment to perform. A much simpler test is the *tension test*.

2.1.1 Experimental Stress-Strain Relations

Tension Tests

Of all mechanical tests for structural materials, the tension test is the most common. This is true primarily because it is a relatively rapid test and requires simple apparatus. It is not as simple to interpret the data it gives, however, as might appear at first sight. J. J. Gilman [1969]

The tensile test [is] very easily and quickly performed but it is not possible to do much with its results, because one does not know what they really mean. They are the outcome of a number of very complicated physical processes. . . . The extension of a piece of metal [is] in a sense more complicated than the working of a pocket watch and to hope to derive information about its mechanism from two or three data derived from measurement during the tensile test [is] perhaps as optimistic as would be an attempt to learn about the working of a pocket watch by determining its compressive strength. E. Orowan [1944]

Despite these caveats, the tension test remains the preferred method of determining the material properties of metals and other solids on which it is easily performed: glass, hard plastics, textile fibers, biological tissues, and many others.

Stress-Strain Diagrams

The immediate result of a tension test is a relation between the axial force and either the change in length (elongation) of a gage portion of the specimen or a representative value of longitudinal strain as measured by one or more strain gages. This relation is usually changed to one between the stress σ (force F divided by cross-sectional area) and the strain ε (elongation divided by gage length or strain-gage output), and is plotted as the *stress-strain diagram*. Parameters that remain constant in the course of a test include the temperature and the rate of loading or of elongation. If significant changes in length and area are attained, then it is important to specify whether the area used in calculating the stress is the original area A_0 (*nominal* or “engineering” stress, here to be denoted simply σ_e) or the current area A (*true* or *Cauchy* stress, σ_t) — in other words, whether the Lagrangian or the Eulerian definition is used — and whether the strain plotted is the change in length Δl divided by the original length l_0 (*conventional* or “engineering” strain, ε_e) or the natural logarithm of the ratio of the current length l ($= l_0 + \Delta l$) to l_0 (*logarithmic* or *natural* strain, ε_l).

Examples of stress-strain diagrams, both as σ_e versus ε_e and as σ_t versus ε_l , are shown in Figure 2.1.1. It is clear that the Cauchy stress, since it does not depend on the initial configuration, reflects the actual state in the specimen better than the nominal stress, and while both definitions of strain involve the initial length, the rates (time derivatives) of conventional and

logarithmic strain are respectively \dot{l}/l_0 and \dot{l}/l , so that it is the latter that is independent of initial configuration. In particular, in materials in which it is possible to perform a compression test analogous to a tension test, it is often found that the stress-strain diagrams in tension and compression coincide to a remarkable degree when they are plots of Cauchy stress against logarithmic strain [see Figure 2.1.1(b)].

The rate of work done by the force is $F\dot{l} = \sigma_e A_0 l_0 \dot{\epsilon}_e = \sigma_t A l \dot{\epsilon}_l$, so that $\sigma_e \dot{\epsilon}_e$ and $\sigma_t \dot{\epsilon}_l$ are the rates of work per unit original and current volume, respectively. While the calculation of Cauchy stress requires, strictly speaking, measurement of cross-sectional area in the course of the test, in practice this is not necessary if the material is a typical one in which the volume does not change significantly, since the current area may be computed from the volume constancy relation $Al = A_0 l_0$.

As is shown in Chapter 8, the logarithmic strain rate $\dot{\epsilon}_l$ has a natural and easily determined extension to general states of deformation, but the logarithmic strain itself does not, except in situations (such as the tension test) in which the principal strain axes are known and remain fixed. The use of the logarithmic strain in large-deformation problems with rotating principal strain axes may lead to erroneous results.

Compression Tests

As seen in Figure 2.1.1(b), the results of a simple compression test on a specimen of ductile metal are virtually identical with those of a tensile test if Cauchy stress is plotted against logarithmic strain. The problem is that a “simple compression test” is difficult to achieve, because of the friction that is necessarily present between the ends of the specimen and the pressure plates. Compression of the material causes an increase in area, and therefore a tendency to slide outward over the plates, against the shear stress on the interfaces due to the frictional resistance. Thus the state of stress cannot be one of simple compression. Lubrication of the interface helps the problem, as does the use of specimens that are reasonably slender — though not so slender as to cause buckling — so that, at least in the middle portion, a state of simple compressive stress is approached.

Unlike ductile metals, brittle solids behave quite differently in tension and compression, the highest attainable stress in compression being many times that in tension. Classically brittle solids, such as cast iron or glass, fracture almost immediately after the proportional limit is attained, as in Figure 2.1.1(c). Others, however, such as concrete and many rocks, produce stress-strain diagrams that are qualitatively similar to those of many ductile materials, as in Figure 2.1.1(d). Of course, the strain scale is quite different: in brittle materials the largest strains attained rarely exceed 1%. The stress peak represents the onset of fracture, while the decrease in slope of the stress-strain curve represents a loss in stiffness due to progressive crack-

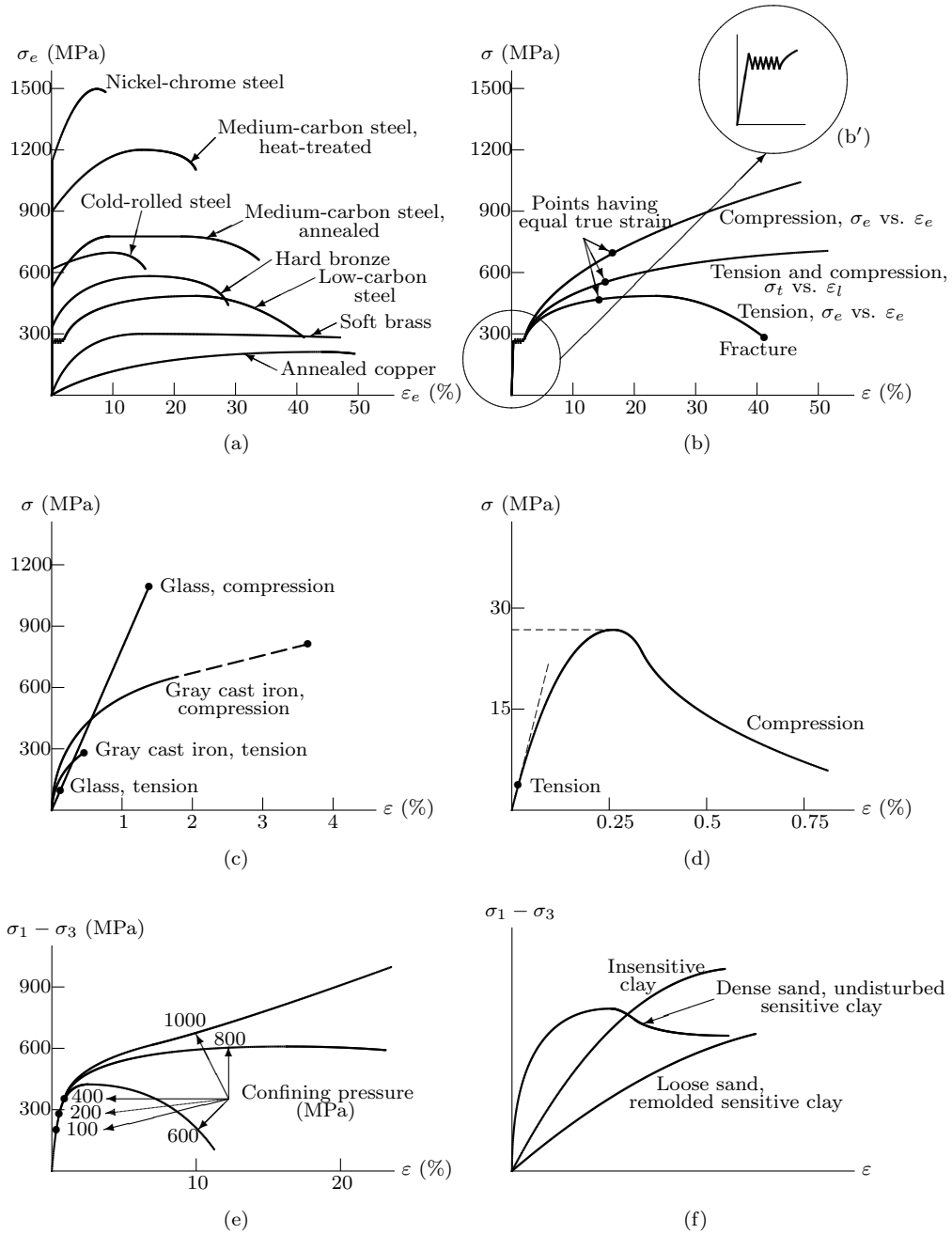


Figure 2.1.1. Stress-strain diagrams: (a) ductile metals, simple tension; (b) ductile metal (low-carbon steel), simple tension and compression; (b') yield-point phenomenon; (c) cast iron and glass, simple compression and tension; (d) typical concrete or rock, simple compression and tension; (e) rock (limestone), triaxial compression; (f) soils, triaxial compression.

ing. The post-peak portion of the curve is highly sensitive to test conditions and specimen dimensions, and therefore it cannot be regarded as a material property. Moreover, it is not compression per se that brings about fracture, but the accompanying shear stresses and secondary tensile stresses. Nevertheless, the superficial resemblance between the curves makes it possible to apply some concepts of plasticity to these materials, as discussed further in Section 2.3.

Unless the test is performed very quickly, soils are usually too soft to allow the use of a compression specimen without the application of a *confining pressure* to its sides through air or water pressure. This *confined compression test* or *triaxial shear test* is frequently applied to rock and concrete as well, for reasons discussed in Section 2.3. The specimen in this test is in an axisymmetric, three-dimensional stress state, the principal stresses being the longitudinal stress σ_1 and the confining pressure $\sigma_2 = \sigma_3$, both taken conventionally as **positive in compression**, in contrast to the usual convention of solid mechanics. The results are usually plotted as $\sigma_1 - \sigma_3$ (which, when positive — as it usually is — equals $2\tau_{\max}$) against the compressive longitudinal strain ε_1 ; typical curves are shown in Figure 2.1.1(e) and (f).

Elastic and Proportional Limits, Yield Strength

Some of the characteristic features of tensile stress-strain diagrams for ductile solids when rate sensitivity may be neglected will now be described. Such diagrams are characterized by a range of stress, extending from zero to a limiting stress (say σ_o) in which the stress is proportional to strain (the corresponding strains are normally so small that it does not matter which definitions of stress and strain are used); σ_o is called the *proportional limit*. Also, it is found that the same proportionality obtains when the stress is decreased, so that the material in this range is linearly elastic, described by the uniaxial Hooke's law given by Equation (1.4.12), that is, $\sigma = E\varepsilon$. The range of stress-strain proportionality is thus also essentially the *elastic range*, and the proportional limit is also the *elastic limit* as defined in Section 1.5.

When the specimen is stressed slightly past the elastic limit and the stress is then reduced to zero, the strain attained at the end of the process is, as a rule, different from zero. The material has thus acquired a *permanent strain*.

Rate effects, which are more or less present in all solids, can distort the results. The “standard solid” model of viscoelasticity discussed in 1.5.1, for example, predicts that in a test carried out at a constant rate of stressing or of straining, the stress-strain diagram will be curved, but no permanent strain will be present after stress removal; the complete loading-unloading diagram presents a hysteresis loop. The curvature depends on the test rate; it is negligible if the time taken for the test is *either very long or very short* compared with the characteristic time τ of the model.

Even in the absence of significant rate effects, it is not always easy to determine an accurate value for the elastic or proportional limit. Some materials, such as soft copper, present stress-strain curves that contain no discernible straight portions. In others, such as aluminum, the transition from the straight to the curved portion of the diagram is so gradual that the determination of the limit depends on the sensitivity of the strain-measuring apparatus. For design purposes, it has become conventional to define as the “yield strength” of such materials the value of the stress that produces a *specified* value of the “offset” or conventional permanent strain, obtained by drawing through a given point on the stress-strain curve a straight line whose slope is the elastic modulus E (in a material such as soft copper, this would be the slope of the stress-strain curve at the origin). Typically used values of the offset are 0.1%, 0.2% and 0.5%. When this definition is used, it is necessary to specify the offset, and thus we would speak of “0.2% offset yield strength.”

2.1.2 Plastic Deformation

Plastic Strain, Work-Hardening

The strain defined by the offset may be identified with the inelastic strain as defined in 1.5.1. In the context in which rate sensitivity is neglected, this strain is usually called the *plastic strain*, and therefore, if it is denoted ε^p , it is given by

$$\varepsilon^p = \varepsilon - \frac{\sigma}{E}. \quad (2.1.1)$$

The plastic strain at a given value of the stress is often somewhat different from the permanent strain observed when the specimen is unloaded from this stress, because the stress-strain relation in unloading is not always ideally elastic, whether as a result of rate effects or other phenomena (one of which, the **Bauschinger effect**, is discussed below).

Additional plastic deformation results as the stress is increased. The stress-strain curve resulting from the initial loading into the plastic range is called the *virgin curve* or *flow curve*. If the specimen is unloaded after some plastic deformation has taken place and then reloaded, the reloading portion of the stress-strain diagram is, like the unloading portion, approximately a straight line of slope E , more or less up to the highest previously attained stress (that is, the stress at which unloading began). The reloading then follows the virgin curve. Similar results occur with additional unloadings and reloadings. The highest stress attained before unloading is therefore a new yield stress, and the material may be regarded as having been *strengthened* or *hardened* by the plastic deformation (or *cold-working*). The increase of stress with plastic deformation is consequently called *work-hardening* or *strain-hardening*.

The virgin curve of work-hardening solids, especially ones without a sharply defined yield stress, is frequently approximated by the **Ramberg–Osgood formula**

$$\varepsilon = \frac{\sigma}{E} + \alpha \frac{\sigma_R}{E} \left(\frac{\sigma}{\sigma_R} \right)^m, \quad (2.1.2)$$

where α and m are dimensionless constants,¹ and σ_R is a reference stress. If m is very large, then ε^p remains small until σ approaches σ_R , and increases rapidly when σ exceeds σ_R , so that σ_R may be regarded as an approximate yield stress. In the limit as m becomes infinite, the plastic strain is zero when $\sigma < \sigma_R$, and is indeterminate when $\sigma = \sigma_R$, while $\sigma > \sigma_R$ would produce an infinite plastic strain and is therefore impossible. This limiting case accordingly describes a *perfectly plastic* solid with yield stress σ_R .

If the deformation is sufficiently large for the elastic strain to be neglected, then Equation (2.1.2) can be solved for σ in terms of ε :

$$\sigma = C\varepsilon^n, \quad (2.1.3)$$

where $C = \sigma_R(E/\alpha\sigma_R)^n$, and $n = 1/m$ is often called the *work-hardening exponent*. Equation (2.1.3), proposed by Ludwik [1909], is frequently used in applications where an explicit expression for stress as a function of strain is needed. Note that the stress-strain curve representing (2.1.3) has an infinite initial slope. In order to accommodate an elastic range with an initial yield stress σ_E , Equation (2.1.3) is sometimes modified to read

$$\sigma = \begin{cases} E\varepsilon, & \varepsilon \leq \frac{\sigma_E}{E}, \\ \sigma_E \left(\frac{E\varepsilon}{\sigma_E} \right)^n, & \varepsilon \geq \frac{\sigma_E}{E}. \end{cases} \quad (2.1.4)$$

Ultimate Tensile Strength

It must be emphasized that when the strain is greater than a few percent, the distinction between the different types of stress and strain must be taken into account. The decomposition (2.1.1) applies, strictly speaking, to the logarithmic strain. The nature of the stress-strain curve at larger strains is, as discussed above, also highly dependent on whether the stress plotted is nominal or true stress [see Figure 2.1.1(b)]. True stress is, in general, an increasing function of strain until fracture occurs. Since the cross-sectional area of the specimen decreases with elongation, the nominal stress increases more slowly, and at a certain point in the test it begins to decrease. Since, very nearly, $\sigma_e = \sigma_t \exp(-\varepsilon_l)$, it follows that

$$d\sigma_e = (d\sigma_t - \sigma_t d\varepsilon_l) \exp(-\varepsilon_l),$$

¹If m is a number other than an odd integer, then $size - 2(\sigma/\sigma_R)^m$ may be replaced by $size - 2|\sigma/\sigma_R|^{m-1}(\sigma/\sigma_R)$ if the curve is the same for negative as for positive stress and strain.

and therefore the nominal stress (and hence the load) is maximum when

$$\frac{d\sigma_t}{d\varepsilon_l} = \sigma_t.$$

If Equation (2.1.3) is assumed to describe the flow curve in terms of Cauchy stress and logarithmic strain, then the maximum nominal stress can easily be seen to occur when $\varepsilon_l = n$.

The maximum value of nominal stress attained in a tensile test is called the *ultimate tensile strength* or simply the *tensile strength*. When the specimen is extended beyond the strain corresponding to this stress, its weakest portion begins to elongate — and therefore also to thin — faster than the remainder, and so a *neck* will form. Further elongation and thinning of the neck — or *necking* — proceeds at decreasing load, until fracture.

Discontinuous Yielding

The stress-strain curves of certain impurity-containing metals, such as mild steel and nitrogen-containing brass, present a phenomenon known as *discontinuous yielding*. When the initial elastic limit is reached, suddenly a significant amount of stretching (on the order of 1 or 2%, and thus considerably larger than the elastic strain achieved up to that point) occurs at essentially constant stress, of a value equal to or somewhat lower than the initial elastic limit. If the value is the same, then it is called the *yield point* of the material. If it is lower, then it is called the *lower yield point*, while the higher value is called the *upper yield point*. The portion of the stress-strain diagram represented by the constant stress value is called the *yield plateau*, and the drop in stress, if any, that precedes it is called the *yield drop*. Following the plateau, work-hardening sets in, as described above. Figure 2.1.1(b') shows a typical stress-strain diagram for a material with a yield point.

As shown in the figure, the stress on the plateau is not really constant but shows small, irregular fluctuations. They are due to the fact that plastic deformation in this stage is not a homogeneous process but concentrated in discrete narrow zones known as *Lüders bands*, which propagate along the specimen as it is stretched, giving rise to surface marks called *stretcher strains*.

When a specimen of a material with a yield point is loaded into the work-hardening range, unloaded, and reloaded soon after unloading, the virgin curve is regained smoothly as described previously. If, however, some time — of the order of hours — is allowed to elapse before reloading, the yield point recurs at a higher stress level (see Figure 2.1.2). This phenomenon is called *strain aging*.

Bauschinger Effect, Anisotropy

A specimen of a ductile material that has been subjected to increasing

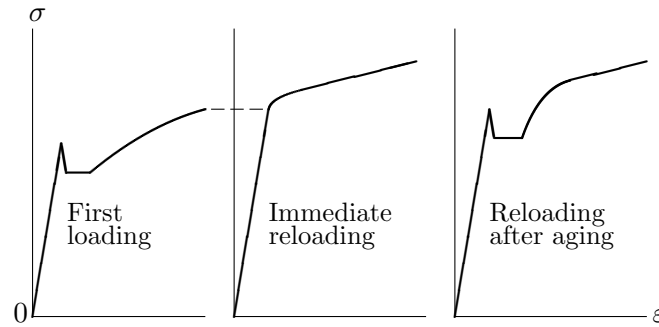


Figure 2.1.2. Strain aging

tensile stress and then unloaded (“cold-worked”) is different from a virgin specimen. We already know that it has a higher tensile yield stress. If, however, it is now subjected to increasing *compressive* stress, it is found that the yield stress in compression is *lower* than before. This observation is known as the **Bauschinger effect** [see Figure 2.1.3(a)].

The Bauschinger effect can be observed whenever the direction of straining is reversed, as, for example, compression followed by tension, or shearing (as in a torsion test on a thin-walled tube) followed by shearing in the opposite direction. More generally, the term “Bauschinger effect” can be used to describe the lowering of the yield stress upon reloading that follows unloading, even if the reloading is in the same direction as the original loading (Lubahn and Felgar [1961]) [see Figure 2.1.3(b)]. Note the hysteresis loop which appears with large strains, even at very slow rates of straining at which the viscoelastic effects mentioned above may be neglected.

Another result of plastic deformation is the loss of isotropy. Following cold-working in a given direction, differences appear between the values of the tensile yield strength in that direction and in a direction normal to it. These differences may be of the order of 10%, but are usually neglected in practice.

Annealing, Recovery

The term “cold-working” used in the foregoing discussions refers to plastic deformation carried out at temperatures below the so-called *recrystallization temperature* of the metal, typically equal, in terms of absolute temperature, to some 35 to 50% of the melting point (although, unlike the melting point, it is not sharply defined); the reason for the name is explained in the next section. The effects of cold-working, such as work-hardening, the Bauschinger effect, and induced anisotropy, can largely be removed by a process called *annealing*, consisting of heating the metal to a relatively high temperature (above the recrystallization temperature) and holding it there for

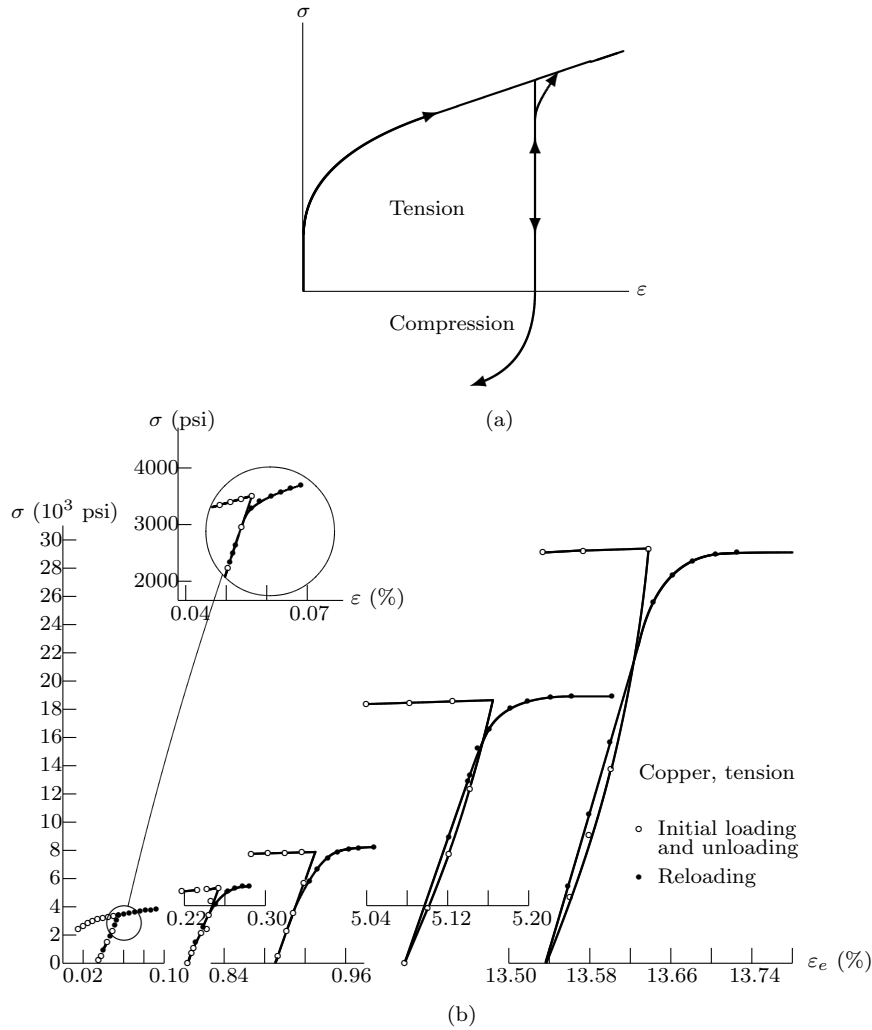


Figure 2.1.3. Bauschinger effect: (a) classical; (b) generalized (from Lubahn and Felgar [1961]).

a certain length of time before slowly cooling it. The length of time necessary for the process decreases with the annealing temperature and with the amount of cold work.

Plastic deformation that takes place at temperatures in the annealing range (i.e., above the recrystallization temperature) is known as *hot-working*, and does not produce work-hardening, anisotropy, or the Bauschinger effect. For metals with low melting points, such as lead and tin, the recrystallization temperature is about 0°C and therefore deformation at room temperature must be regarded as hot-working. Conversely, metals with very high melting points, such as molybdenum and tungsten (with recrystallization temperatures of 1100 to 1200°C) can be “cold-worked” at temperatures at which the

metal is red-hot.

The recrystallization temperature provides a qualitative demarcation between stress-strain diagrams that show work-hardening and those that do not. Within each of the two ranges, however, the stress needed to achieve a given plastic deformation at a given strain rate also depends on the temperature. In particular, it decreases with increasing temperature (see Figure 2.1.4).

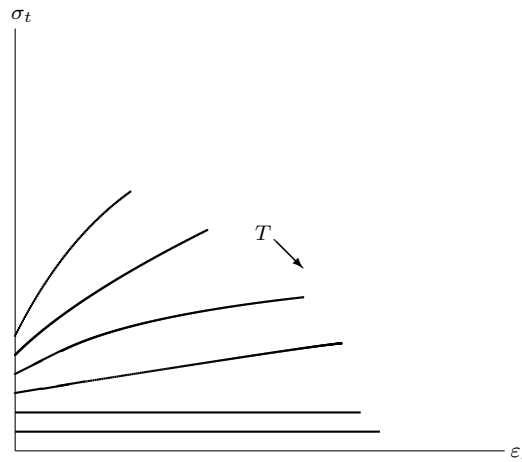


Figure 2.1.4. Temperature dependence of flow stress

A characteristic of some metals (including mild steel), with important implications for design, is a change of behavior from ductile to brittle when the temperature falls below the so-called *transition temperature*.

Softening (that is, a spontaneous decrease in yield strength) of work-hardened metals also occurs at temperatures below recrystallization. This process, whose rate is considerably slower than that of annealing, is called *recovery*. The rate of recovery decreases with decreasing temperature, and is negligible at room temperature for such metals as aluminum, copper and steel. These metals may accordingly be regarded for practical purposes as work-hardening permanently.

2.1.3 Temperature and Rate Dependence

The preceding discussion of the rates of annealing and recovery shows the close relationship between temperature and rate. A great many physico-chemical rate processes — specifically, those that are *thermally activated* — are governed by the **Arrhenius equation**, which has the general form

$$\text{rate} \propto e^{-\Delta E/kT}, \quad (2.1.5)$$

where k is Boltzmann's constant (1.38×10^{-23} J/K), T is the absolute temperature, and ΔE is the *activation energy* of the process. The rate sensitivity of the work-hardening stress-strain curve itself increases with increasing temperature. In a good many metals, the dependence on the plastic strain rate of the stress required to achieve a given plastic strain can be approximated quite well by $\dot{\epsilon}^r$, where the exponent r (sometimes called simply the rate sensitivity) depends on the plastic strain and the temperature, increasing with both. Some typical results for r , obtained from tests at strain rates between 1 and 40 per second, are shown in Table 2.1.1.

Table 2.1.1

Metal	Temperature (°C)	Value of r for a compression of		
		10%	30%	50%
Aluminum	18	0.013	0.018	0.020
	350	0.055	0.073	0.088
	550	0.130	0.141	0.155
Copper	18	0.001	0.002	0.010
	450	0.001	0.008	0.031
	900	0.134	0.154	0.190
Mild steel	930	0.088	0.094	0.105
	1200	0.116	0.141	0.196

Source: Johnson and Mellor [1973].

The Arrhenius equation (2.1.5) permits, in principle, the simultaneous representation of the rate sensitivity and temperature sensitivity of the stress-strain relation by means of the parameter $\dot{\epsilon} \exp(\Delta E/RT)$, or, more generally, $\dot{\epsilon} f(T)$, where $f(T)$ is an experimentally determined function, since the activation energy ΔE may itself be a function of the temperature.

Creep

The preceding results were obtained from tests carried out at constant strain rate (since the strains are large, total and plastic strain need not be distinguished). Following Ludwik [1909], it is frequently assumed that at a given temperature, a relation exists among stress, plastic (or total) strain, and plastic (or total) strain rate, independently of the process, and therefore this relation also describes *creep*, that is, continuing deformation at constant stress. Such a relation is reminiscent of the “standard solid” model of viscoelasticity, in which this relation is linear. It will be recalled that this model describes both the rate dependence of the stress-strain relation (discussed above in this section) and the increasing deformation at constant stress known as creep, which in this case asymptotically attains a finite value (*bounded creep*), though in the limiting case of the Maxwell model it becomes steady creep. In fact, all linear spring-dashpot models of viscoelasticity lead

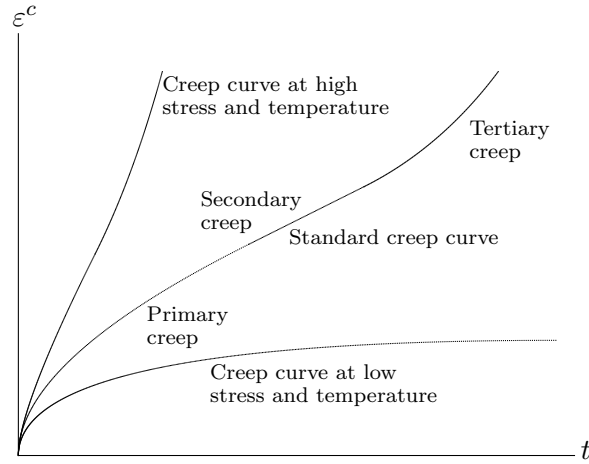


Figure 2.1.5. Typical creep curves for metals.

to creep that is either bounded or steady.

For metals, the relation, if it exists, is nonlinear — many different forms have been proposed — and therefore the resulting creep need not belong to one of the two types predicted by the linear models. Typical creep curves for a metal, showing the creep strain ε^c (equal to the total strain less the initial strain) as a function of time at constant stress and temperature, are shown in Figure 2.1.5. The standard curve is conventionally regarded as consisting of three stages, known respectively as primary (or transient), secondary (or steady), and tertiary (or accelerating) creep, though not all creep curves need contain all three stages. At low stresses and temperatures, the primary creep resembles the bounded creep of linear viscoelasticity, with a limiting value attained asymptotically, and secondary and tertiary creep never appear. At higher stress or temperature, however, the primary creep shows a logarithmic or a power dependence on time:

$$\varepsilon^c \propto \ln t \quad \text{or} \quad \varepsilon^c \propto t^\alpha,$$

where α is between 0 and 1, a frequently observed value being $\frac{1}{3}$ (**Andrade's creep law**). The logarithmic form is usually found to prevail below, and the power form above, the recrystallization temperature.

Creep described by the power law can be derived from a formula relating stress, creep strain and creep-strain rate that has the form (due to Nadai [1950])

$$\sigma = C(\varepsilon^c)^n(\dot{\varepsilon}^c)^r, \quad (2.1.6)$$

where C , n , and r depend on the temperature; this formula reduces to the Ludwik equation (2.1.3) at constant strain rate, and implies a rate sensitivity

that is independent of the strain. At constant stress, the equation can be integrated, resulting in a power law with $\alpha = r/(n + r)$.

Tertiary (accelerating) creep is generally regarded as resulting from structural changes leading to a loss of strength and, eventually, fracture. Whether secondary (steady) creep really takes place over a significant time interval, or is merely an approximate description of creep behavior near an inflection point of the creep curve, is not certain (see Lubahn and Felgar [1961], pp. 136–141). In either case, however, one may speak of a *minimum creep rate* characteristic of the metal at a given stress and temperature, if these are sufficiently high. At a given stress, the temperature dependence of this minimum creep rate is usually found to be given fairly closely by the Arrhenius equation. Its dependence on stress at a given temperature can be approximated by an exponential function at higher stresses, and by a power function of the form $\dot{\varepsilon}_{\min}^c \propto \sigma^q$, where q is an exponent greater than 1 (the frequently used **Bailey–Norton law**), at lower stresses. (Note that Equation (2.1.6) describes the Bailey–Norton law if $n = 0$ and $r = 1/q$.) A commonly used approximation for the creep strain as a function of time, at a given stress and temperature, is

$$\varepsilon^c(t) = \varepsilon_0^c + \dot{\varepsilon}_{\min}^c t,$$

where $\dot{\varepsilon}_{\min}^c$ is the minimum creep rate, and ε_0^c is a fictitious initial value defined by the ε^c -intercept of the straight line tangent to the actual creep curve at the point of inflection or in the steady-creep portion.

In many materials at ordinary temperatures, rate-dependent inelastic deformation is insignificant when the stress is below a yield stress. A simple model describing this effect is the **Bingham model**:

$$\dot{\varepsilon}^i = \begin{cases} 0, & |\sigma| < \sigma_Y, \\ \left(1 - \frac{\sigma_Y}{|\sigma|}\right) \frac{\sigma}{\eta}, & |\sigma| \geq \sigma_Y, \end{cases} \quad (2.1.7)$$

where η is a viscosity, and the yield stress σ_Y may depend on strain. The Bingham model is the simplest model of **viscoplasticity**. Its generalizations are discussed in Section 3.1.

Exercises: Section 2.1

1. Show that the relation between the conventional strain ε_e and the logarithmic strain ε_l is $\varepsilon_l = \ln(1 + \varepsilon_e)$.
2. It is assumed that the stress-strain relations of isotropic linear elasticity, with Young's modulus E and Poisson's ratio ν , are exact in terms of true stress and logarithmic strain. For uniaxial stress, find the relation (parametric if necessary) between the conventional stress and the

conventional strain. Show that the second-order approximation to the relation is $\sigma_e = E[\varepsilon_e - (\frac{1}{2} + 2\nu)\varepsilon_e^2]$.

3. A uniaxial tension test produces a curve of true stress against logarithmic strain that is fitted by $\sigma_t = 2 \times 10^5 \varepsilon_l$ in the elastic range and $\sigma_t = 635 \varepsilon_l^{1/6}$ in the plastic range, with stresses in MPa. Determine (a) the elastic-limit stress, (b) the logarithmic and conventional strains at maximum load, and (c) the true and conventional stresses at maximum load, assuming negligible volume change.
4. If the reference stress σ_R in the Ramberg–Osgood formula (2.1.2) is the offset yield strength for a given permanent strain ε_R , find α in terms of σ_R , ε_R , and E .
5. Find a formula describing a stress-strain relation that (a) is linear for $\sigma < \sigma_E$, (b) asymptotically tends to $\varepsilon \propto \sigma^m$, and (c) is smooth at $\sigma = \sigma_E$.
6. Suppose that in Equation (2.1.6) only C depends on the temperature. Show that, for a given stress, the creep curves corresponding to different temperatures are parallel if they are plotted as creep strain against the logarithm of time.
7. Determine the form of the creep law resulting from Equation (2.1.6).
8. Assuming $\varepsilon = \sigma/E + \varepsilon^c$, and letting $n = 0$ in Equation (2.1.6), determine the resulting relaxation law, i. e. σ as a function of t when a strain ε is suddenly imposed at $t = 0$ and maintained thereafter.
9. To what does the Bingham model described by Equation (2.1.7) reduce when $\sigma_Y = 0$? When $\eta = 0$?

Section 2.2 Crystal Plasticity

2.2.1 Crystals and Slip

Crystal Structure

Plasticity theory was developed primarily in order to describe the behavior of ductile metals. Metals in their usual form are *polycrystalline aggregates*, that is, they are composed of large numbers of grains, each of which has the structure of a simple crystal.

A crystal is a three-dimensional array of atoms forming a regular lattice; it may be regarded as a molecule of indefinite extent. The atoms vibrate

about fixed points in the lattice but, by and large, do not move away from them, being held more or less in place by the forces exerted by neighboring atoms. The forces may be due to ionic, covalent, or metallic bonding. Ionic bonds result from electron transfer from electropositive to electronegative atoms, and therefore can occur only in compounds of unlike elements. Ionic crystal structures range from very simple, such as the sodium chloride structure in which Na^+ and Cl^- alternate in a simple cubic array, to the very complex structures found in ceramics. Covalent bonds are due to the sharing of electrons, and are found in diamond and, to some extent, in crystalline polymers.

In a metallic crystal, the outer or valence electrons move fairly freely through the lattice, while the “cores” (consisting of the nucleus and the filled shells of electrons) vibrate about the equilibrium positions. The metallic bond is the result of a rather complex interaction among the cores and the “free” electrons. It is the free electrons that are responsible for the electrical and thermal conductivity of metals.

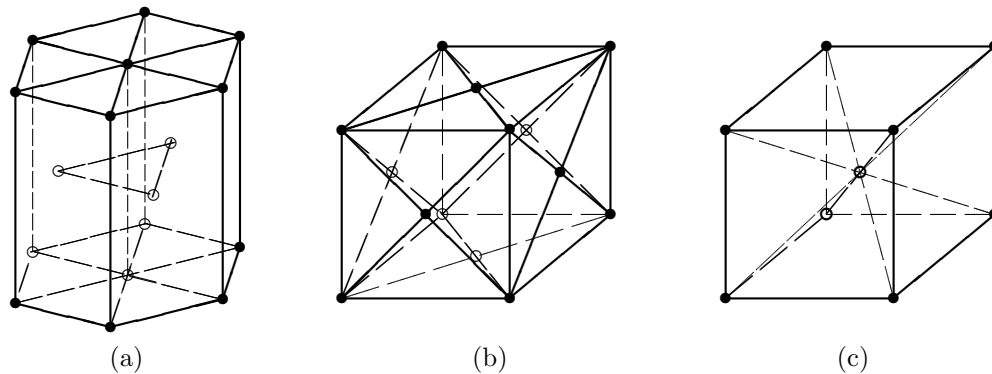


Figure 2.2.1. Crystal structures: (a) hexagonal close-packed (hcp); (b) face-centered cubic (fcc); (c) body-centered cubic (bcc).

The most common crystal structures in metals are the hexagonal close-packed (hcp), face-centered cubic (fcc) and body-centered cubic (bcc), shown in Figure 2.2.1. Because of the random orientation of individual grains in a typical metallic body, the overall behavior of the aggregate is largely isotropic, but such phenomena as the Bauschinger effect and preferred orientation, which occur as a result of different plastic deformation of grains with different orientations, demonstrate the effect of crystal structure on plastic behavior. It is possible, however, to produce specimens of crystalline solids — not only metals — in the form of *single crystals* of sufficiently large size to permit mechanical testing.

Crystal Elasticity

The linear elastic behavior of a solid is described by the elastic modulus matrix \underline{C} defined in 1.4.2. The most general anisotropic solid has 21 inde-

pendent elements of \underline{C} . For the isotropic solid, on the other hand, the only nonzero elements of \underline{C} are (a) $C_{11} = C_{22} = C_{33}$, (b) $C_{44} = C_{55} = C_{66}$, and (c) $C_{12} = C_{13} = C_{23}$ (the symmetry $C_{IJ} = C_{JI}$ is not explicitly shown). But only two of the three values are independent, since $C_{11} = \lambda + 2\mu$, $C_{44} = \mu$, and $C_{12} = \lambda$, so that

$$C_{44} = \frac{1}{2}(C_{11} - C_{12}).$$

In a crystal with cubic symmetry (such as simple cubic, fcc or bcc), with the Cartesian axes oriented along the cube edges, the nonzero elements of \underline{C} are the same ones as for the isotropic solid, but the three values C_{11} , C_{12} and C_{44} are independent. It may, of course, happen fortuitously that the isotropy condition expressed by the preceding equation is satisfied for a given cubic crystal; this is the case for tungsten.

A crystal with hexagonal symmetry is isotropic in the basal plane. Thus, if the basal planes are parallel to the x_1x_2 -plane, $C_{66} = \frac{1}{2}(C_{11} - C_{12})$. The following elements of \underline{C} are independent: (a) $C_{11} = C_{22}$, (b) C_{33} , (c) C_{12} , (d) $C_{13} = C_{23}$, and (e) $C_{44} = C_{55}$.

The anisotropy of crystals is often studied by performing tension tests on specimens with different orientations, resulting in orientation-dependent values of the Young's modulus E . If the maximum and minimum values are denoted E_{\max} and E_{\min} , respectively, while E_{ave} denotes the polycrystalline average, the *anisotropy index* may be defined as $(E_{\max} - E_{\min})/E_{\text{ave}}$. Values range widely: 1.13 for copper, 0.73 for α -iron, 0.2 for aluminum, and, as indicated above, zero for tungsten.

Crystal Plasticity

Experiments show that plastic deformation is the result of relative motion, or *slip*, on specific crystallographic planes, in response to shear stress along these planes. It is found that the *slip planes* are most often those that are parallel to the planes of closest packing; a simple explanation for this is that the separation between such planes is the greatest, and therefore slip between them is the easiest, since the resistance to slip as a result of interatomic forces decreases rapidly with interatomic distance. Within each slip plane there are in turn preferred *slip directions*, which once more are those of the atomic rows with the greatest density, for the same reason. A slip plane and a slip direction together are said to form a *slip system*.

In hcp crystals, which include zinc and magnesium, the planes of closest packing are those containing the hexagons, and the slip directions in those planes are parallel to the diagonals. Hexagonal close-packed crystals therefore have three primary slip systems, although at higher temperatures other, secondary, slip systems may become operative.

Face-centered cubic crystals, by contrast, have twelve primary slip systems: the close-packed planes are the four octahedral planes, and each con-

tains three face diagonals as the closest-packed lines. As a result, fcc metals, such as aluminum, copper, and gold, exhibit considerably more ductility than do hcp metals.

In body-centered cubic crystals there are six planes of closest packing and two slip directions in each, for a total of twelve primary slip systems. However, the difference in packing density between the closest-packed planes and certain other planes is not great, so that additional slip systems become available even at ordinary temperatures. Consequently, metals having a bcc structure, such as α -iron (the form of iron found at ordinary temperatures), tungsten, and molybdenum, have a ductility similar to that of fcc metals.

The preceding correlation between ductility and lattice type is valid in very broad terms. Real metal crystals almost never form perfect lattices containing one type of atom only; they contain imperfections such as geometric lattice defects and impurity atoms, besides the grain boundaries contained in polycrystals. In fact, these imperfections are the primary determinants of crystal plasticity. Ductility must therefore be regarded as a *structure-sensitive* property, as are other inelastic properties. It is only the thermoelastic properties discussed in 1.4.1 — the elastic moduli, thermal stress (or strain) coefficients, and specific heat — that are primarily influenced by the ideal lattice structure, and are therefore called *structure-insensitive*.

Slip Bands

In principle, slip in a single crystal can occur on every potential slip plane when the necessary shear stress is acting. Observations, however, show slip to be confined to discrete planes.¹ When a slip plane intersects the outer surface, an observable *slip line* is formed, and slip lines form clusters called *slip bands*. In a given slip band, typically, a new slip line forms at a distance of the order of 100 interatomic spacings from the preceding one when the amount of slip on the latter has reached something of the order of 1,000 interatomic spacings. It follows from these observations that slip does not take place by a uniform relative displacement of adjacent atomic planes.

Critical Resolved Shear Stress

It was said above that slip along a slip plane occurs in response to shear stress on that plane. In particular, in a tensile specimen of monocrystalline metal in which the tensile stress σ acts along an axis forming an angle ϕ with the normal to the slip plane and an angle λ with the slip direction, then the relation between σ and the resolved shear stress on the slip plane and in the slip direction, τ , is

$$\sigma = (\cos \phi \cos \lambda)^{-1} \tau. \quad (2.2.1)$$

It was found by Schmid [1924], and has been confirmed by many experiments,

¹Or, more generally, surfaces (*slip surfaces*), since slip may transfer from one slip plane to another which intersects it in the interior of the crystal, especially in bcc metals.

that slip in a single crystal is initiated when the resolved shear stress on some slip system reaches a critical value τ_c , which is a constant for a given material at a given temperature and is known as the *critical resolved shear stress*. This result is called **Schmid's law**. The critical resolved shear stress is, as a rule, very much higher for bcc metals (iron, tungsten) than for fcc metals (aluminum, copper) or hcp metals (zinc, magnesium).

Theoretical Shear Strength

A value of the shear stress necessary to produce slip may be calculated by assuming that slip takes place by the uniform displacement of adjacent atomic planes. Consider the two-dimensional picture in Figure 2.2.2: two

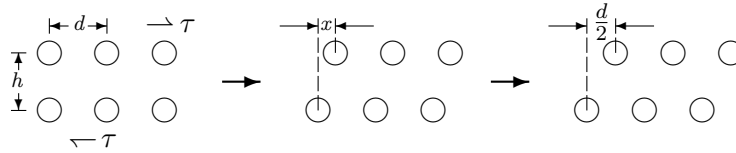


Figure 2.2.2. Slip between two neighboring rows of atoms

neighboring rows of atoms, the distance between the centers of adjacent atoms in each row being d , and the distance between the center lines of the two rows being h . Suppose the two rows to be in a stable equilibrium configuration under zero stress. If one row is displaced by a distance d relative to the other, a new configuration is achieved that is indistinguishable from the first. A displacement of $d/2$, on the other hand, would lead to an unstable equilibrium configuration at zero stress. As a first approximation, then, the shear stress necessary to produce a relative displacement x may be assumed to be given by

$$\tau = \tau_{\max} \sin \frac{2\pi x}{d}, \quad (2.2.2)$$

and slip would proceed when $\tau = \tau_{\max}$. When the displacement x is small, the stress-displacement relation is approximately linear: $\tau = 2\pi\tau_{\max}x/d$. But a small displacement x between rows a distance h apart corresponds to a lattice shear of $\gamma = x/h$, and Hooke's law in shear reads $\tau = G\gamma$ [Equation (1.4.15)]. Consequently,

$$\tau_{\max} = \frac{Gd}{2\pi h}.$$

Since $h \equiv d$, the value $G/6$ is a first, structure-insensitive approximation to the so-called *theoretical shear strength* of a crystal.

More refined calculations that take actual crystal structures into account reduce the value of the theoretical shear strength to about $G/30$. In reality, however, the shear strength of single crystals is less than this by one to three orders of magnitude, that is, it is of order $10^{-3}G$ to $10^{-5}G$. Only in

so-called *whiskers*, virtually perfect crystals about $1\ \mu\text{m}$ in diameter, is a shear strength of the theoretical order of magnitude observed.

2.2.2 Dislocations and Crystal Plasticity

The discrepancy between theoretical and observed shear strength, as well as the observation of slip bands, have led to the inevitable conclusion that slip in ordinary crystals must take place by some mechanism other than the movement of whole planes of atoms past one another, and that it is somehow associated with lattice defects. A mechanism based on a specific defect called a *dislocation* was proposed independently by G. I. Taylor [1934] and E. Orowan [1934].

Defects in Crystals

All real crystals contain defects, that is, deviations from the ideal crystal structure. A defect concentrated about a single lattice point and involving only a few atoms is called a *point defect*; if it extends along a row of many atoms, it is called a *line defect*; and if it covers a whole plane of atoms, a *planar defect*.

Point defects are shown in Figure 2.2.3. They may be purely structural, such as (a) a vacancy or (b) an interstitial atom, or they may involve foreign atoms (*impurities*): (c) a substitutional impurity, (d) an interstitial impurity. As shown in the figure, point defects distort the crystal lattice locally,

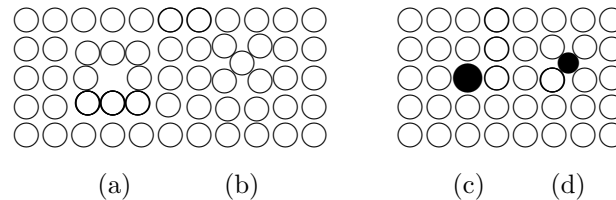


Figure 2.2.3. Point defects: (a) vacancy; (b) interstitial atom; (c) substitutional impurity; (d) interstitial impurity.

the distortion being significant over a few atomic distances but negligible farther away. Planar defects, illustrated in Figure 2.2.4, include (a) grain boundaries in polycrystals, and within single crystals, (b) twin boundaries and (c) stacking faults.

Dislocations

The most important line defects in crystals are *dislocations*. The concept of a dislocation has its origin in continuum mechanics, where it was introduced by V. Volterra. Consider a hollow thick-walled circular cylinder in which a radial cut, extending through the wall, is made [see Figure

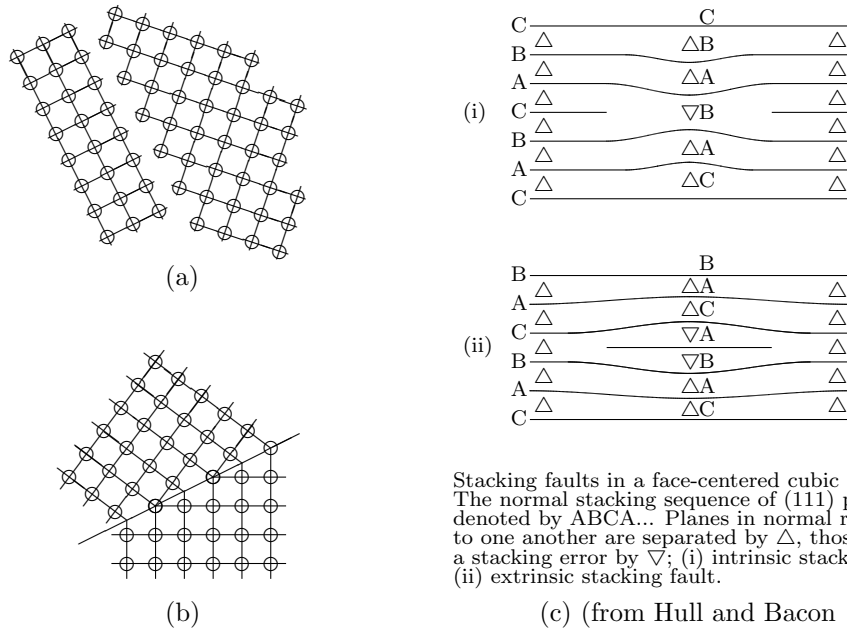


Figure 2.2.4. Planar defects: (a) grain boundary; (b) twin boundary; (c) stacking fault.

2.2.5(a)]. The two faces of the cut may be displaced relative to each other by a distance b , either in the (b) radial or (c) axial direction, and then reattached. The result is a *Volterra dislocation*, with Figures 2.2.5(b) and (c)

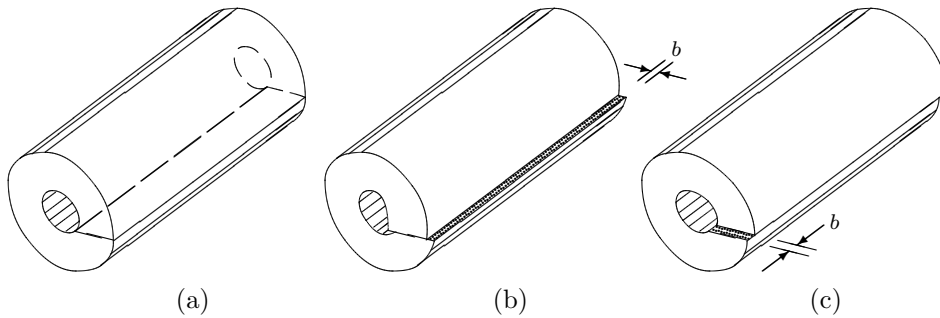


Figure 2.2.5. Volterra dislocation: (a) Volterra cut; (b) edge dislocation; (c) screw dislocation.

representing respectively an *edge* and a *screw* dislocation. When the rough edges are smoothed, the result is a cylinder looking much as it did before the operation, but containing a self-equilibrating internal stress field. If the material is isotropic and linearly elastic, then the stress and displacement fields can be calculated by means of the theory of elasticity. In particular,

the strain energy per unit length of cylinder is found to be

$$W' = \frac{Gb^2}{4\pi(1-\nu)} \left(\ln \frac{R}{a} - 1 \right) \quad (2.2.3a)$$

for an edge dislocation and

$$W' = \frac{Gb^2}{4\pi} \left(\ln \frac{R}{a} - 1 \right) \quad (2.2.3b)$$

for a screw dislocation, where G is the shear modulus, ν is the Poisson's ratio, and R and a are respectively the outer and inner radii of the cylinder.

An edge dislocation in a crystal can be visualized as a line on one side of which an extra half-plane of atoms has been introduced, as illustrated in Figure 2.2.6(a) for a simple cubic lattice. At a sufficient number of atomic distances away from the dislocation line, the lattice is virtually undisturbed. Consider, now, a path through this “good” crystal which would be closed if the lattice were perfect. If such a path, consisting of the same number of atom-to-atom steps in each direction, encloses a dislocation, then, as shown in the figure, it is not closed; the vector \mathbf{b} needed to close it is called the *Burgers vector* of the dislocation, and the path defining it is called the *Burgers circuit*.

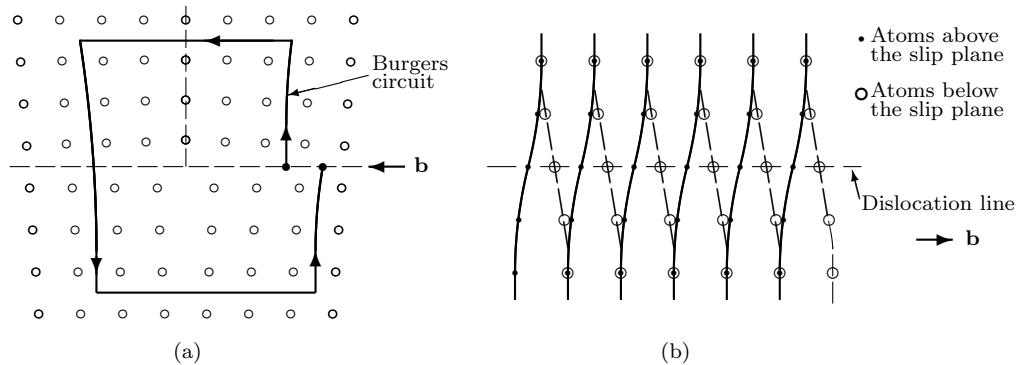


Figure 2.2.6. Dislocation in a crystal: (a) edge dislocation; (b) screw dislocation.

Note that, for an edge dislocation, the Burgers vector is necessarily perpendicular to the dislocation line. Indeed, this can be used as the defining property of an edge dislocation. Similarly, a screw dislocation can be defined as one whose Burgers vector is parallel to the dislocation line [see Figure 2.2.6(b)].

A dislocation in a crystal need not be a straight line. However, the Burgers vector must remain constant. Thus, a dislocation can change from edge

to screw, or vice versa, if it makes a right-angle turn. It cannot, moreover, terminate inside the crystal, but only at the surface of a crystal or at a grain boundary. It can form a closed loop, or branch into other dislocations (at points called *nodes*), subject to the **conservation of the Burgers vectors**: the sum of the Burgers vectors of the dislocations meeting at a node must vanish if each dislocation is considered to go into the node (Frank [1951]).

Dislocations and Slip

It is now universally accepted that plastic deformation in crystals results from the movement of dislocations. As can be seen from Figure 2.2.7, in order

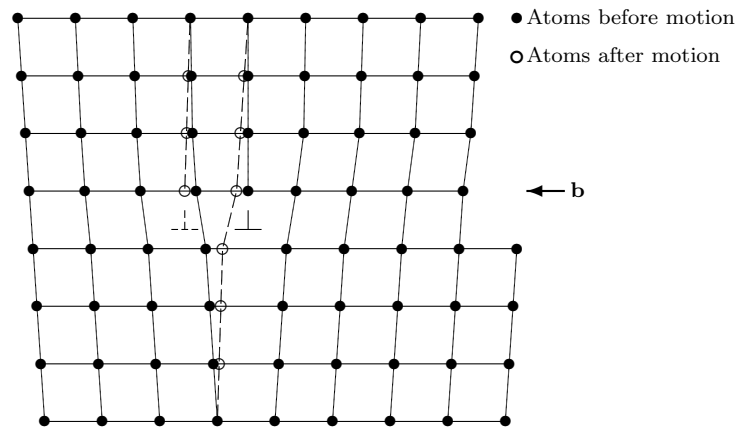


Figure 2.2.7. Slip by means of an edge dislocation.

for an edge dislocation to move one atomic distance in the plane containing it and its Burgers vector (the slip plane), each atom need move only a small fraction of an atomic distance. Consequently, the stress required to move the dislocation is only a small fraction of the theoretical shear strength discussed in 2.2.1. An approximate value of this stress is given by the *Peierls–Nabarro stress*,

$$\tau_{\text{PN}} = \frac{2G}{1-\nu} \exp \left[-\frac{2\pi h}{d(1-\nu)} \right],$$

where h and d denote, as before, the distances between adjacent planes of atoms and between atoms in each plane, respectively. The Peierls–Nabarro stress is clearly much smaller than the theoretical shear strength. Its value, moreover, depends on h/d , and the smallest value is achieved when h/d is largest, that is, for close-packed planes that are as far apart as possible; this result explains why such planes are the likeliest slip planes. When $h = \sqrt{2}d$, τ_{PN} is of the order $10^{-5}G$, consistent with the observed shear strength of pure single crystals.

If the stress is maintained, the dislocation can move to the next position, and the next, and so on. As the dislocation moves in its slip plane, the

portion of the plane that it leaves behind can be regarded as having experienced slip of the amount of one Burgers-vector magnitude $b = |\mathbf{b}|$. When the dislocation reaches the crystal boundary, slip will have occurred on the entire slip plane. Suppose that the length of the slip plane is s , and that an edge dislocation moves a distance x in the slip plane; then it contributes a displacement bx/s , so that n dislocations moving an average distance \bar{x} produce a displacement $u = nb\bar{x}/s$. If the average spacing between slip planes is l , then the plastic shear strain is

$$\gamma^p = \frac{u}{l} = \frac{nb\bar{x}}{ls}.$$

However, n/l is just the average number of dislocation lines per unit perpendicular area, or, equivalently, the total length of dislocation lines of the given family per unit crystal volume — a quantity known as the *density* of dislocations, usually denoted ρ . Since only the mobile dislocations contribute to plastic strain, it is their density, denoted ρ_m , that must appear in the equation for the plastic strain, that is,

$$\gamma^p = \rho_m b \bar{x},$$

and the plastic shear-strain rate is

$$\dot{\gamma}^p = \rho_m b \bar{v},$$

where \bar{v} is the average dislocation velocity.

Forces on and Between Dislocations

A shear stress τ acting on the slip plane and in the direction of the Burgers vector produces a force per unit length of dislocation that is perpendicular to the dislocation line and equal to τb . To prove this result, we consider an infinitesimal dislocation segment of length dl ; as this segment moves by a distance ds , slip of an amount b occurs over an area $dl ds$, and therefore the work done by the shear stress is $(\tau dl ds)b = (\tau b) dl ds$, equivalent to that done by a force $(\tau b)dl$, or τb per unit length of dislocation.

Equations (2.2.3) for the strain energy per unit length of a dislocation in an isotropic elastic continuum may be used to give an order-of-magnitude estimate for the strain energy per unit length of a dislocation in a crystal, namely,

$$W' = \alpha G b^2, \quad (2.2.4)$$

where α is a numerical factor between 0.5 and 1.

Two parallel edge dislocations having the same slip plane have, when they are far apart, a combined energy equal to the sum of their individual energies, that is, $2\alpha G b^2$ per unit length, since any interaction between them is negligible. When they are very close together, then, if they are unlike

(that is, if their Burgers vectors are equal and opposite), they will annihilate each other and the resulting energy will be zero; thus they attract each other in order to minimize the total energy. Like dislocations, on the other hand, when close together are equivalent to a single dislocation of Burgers vector $2\mathbf{b}$, so that the energy per unit length is $\alpha G(2b)^2$, and therefore they repel each other in order to reduce the energy.

Frank–Read Source

The number of dislocations typically present in an unstressed, annealed crystal is not sufficient to produce plastic strains greater than a few percent. In order to account for the large plastic strains that are actually produced, it is necessary for large numbers of dislocations to be created, and on a relatively small number of slip planes, in order to account for slip bands. The *Frank–Read source* is a mechanism whereby a single segment of an edge dislocation, anchored at two interior points of its slip plane, can produce a large number of dislocation loops. The anchor points can be point defects, or points at which the dislocation joins other dislocations in unfavorable planes.

If α in Equation (2.2.4) is constant along the dislocation, independently of its orientation, then an increase ΔL in dislocation length requires an energy increment $W' \Delta L$, that is, work in that amount must be done on it. This is equivalent to assuming that a line tension T equal to W' is acting along the dislocation. In order to deform an initially straight dislocation segment into a circular arc subtending an angle 2θ , equilibrium requires a restoring force $F = 2T \sin \theta$ perpendicular to the original dislocation segment. If the length of the segment is L , then the force per unit length is F/L and can be produced by a shear stress $\tau = F/bL$, or

$$\tau = \frac{2\alpha Gb}{L} r \sin \theta.$$

When $\theta = \pi/2$, that is, when the dislocation segment forms a semicircle, the shear stress is maximum and equal to

$$\tau_{\max} = \frac{Gb}{L}$$

if $\alpha = 0.5$, as it is frequently taken.

If the maximum necessary shear stress is acting on a dislocation segment pinned at two points, as in Figure 2.2.8, the semicircular form is soon attained, whereupon the dislocation becomes unstable and expands indefinitely. The expanding loop doubles back on itself, as in (c) and (d), until two sections meet and annihilate each other, since they have the same Burgers vector but opposite line sense, forming a closed outer loop that continues to expand and a new dislocation segment that will repeat the process.

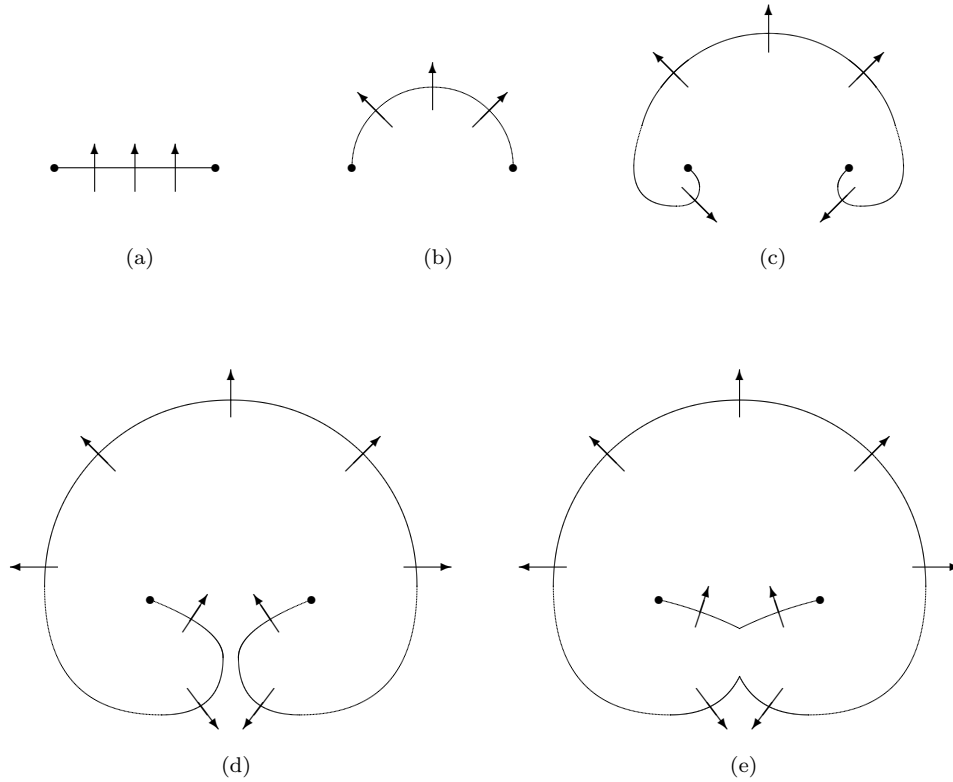


Figure 2.2.8. Frank–Read source (after Read [1953]).

Other mechanisms for the multiplication of dislocations that are similar to the Frank–Read source involve screw dislocations and include *cross-slip* and the *Bardeen–Herring source* (see, e.g., Hull and Bacon [1984]).

2.2.3 Dislocation Models of Plastic Phenomena

W. T. Read, Jr., in his classic *Dislocations in Crystals* (Read [1953]), offered the following caution: “Little is gained by trying to explain any and all experimental results by dislocation theory; the number of possible explanations is limited only by the ingenuity, energy, and personal preference of the theorist.”

Indeed, much theoretical work has been expended in the past half-century in attempts to explain the phenomena of metal plasticity, discussed in Section 2.1, by means of dislocation theory. No comprehensive theory has been achieved, but numerous qualitative or semi-quantitative explanations have been offered, and some of these are now generally accepted. A few are described in what follows.

Yield Stress

If the loops generated by Frank–Read sources or similar mechanisms could all pass out of the crystal, then an indefinite amount of slip could be produced under constant stress. In reality, obstacles to dislocation movement are present. These may be scattered obstacles such as impurity atoms or precipitates, extended barriers such as grain boundaries, or other dislocations that a moving dislocation has to intersect (“forest dislocations”). In addition, if a dislocation is stopped at a barrier, then successive dislocations emanating from the same Frank–Read source pile up behind it, stopped from further movement by the repulsive forces that like dislocations exert on one another.

The yield stress is essentially the applied shear stress necessary to provide the dislocations with enough energy to overcome the short-range forces exerted by the obstacles as well as the long-range forces due to other dislocations. The mechanisms are many and complex, and therefore there is no single dislocation theory of the yield strength but numerous theories attempting to explain specific phenomena of metal plasticity. This is especially true for alloys, in which the impurity atoms may present various kinds of obstacles, depending on the form they take in the host lattice — for example, whether as solutes or precipitates (for a general review, see, e.g., Nabarro [1975]).

Yield Point

Under some conditions, solute atoms tend to segregate in the vicinity of a dislocation at a much greater density than elsewhere in the lattice, forming so-called *Cottrell atmospheres*. In order to move the dislocation, an extra stress is required to overcome the anchoring force exerted on it by the solutes. Once the dislocation is dislodged from the atmosphere, however, the extra stress is no longer necessary, and the dislocation can move under a stress that is lower than that required to initiate the motion. This is the explanation, due to Cottrell and Bilby [1949], of the yield-point phenomenon discussed in 2.1.2 [see Figure 2.1.1(b’)]. Strain-aging (Figure 2.1.2) is explained by the fact that the formation of atmospheres takes place by diffusion and is therefore a rate process. Thus if a specimen is unloaded and immediately reloaded, not enough time will have passed for the atmospheres to form anew. After a sufficient time, whose length decreases with increasing temperature, the solutes segregate once more and the upper yield point returns.

Work-Hardening

As plastic deformation proceeds, dislocations multiply and eventually get stuck. The stress field of these dislocations acts as a *back stress* on mobile dislocations, whose movement accordingly becomes progressively more difficult, and an ever greater applied stress is necessary to produce additional

plastic deformation. This is the phenomenon of work-hardening.

In a first stage, when only the most favorably oriented slip systems are active, the back stress is primarily due to interaction between dislocations on parallel slip planes and to the pile-up mechanism. In this stage work-hardening is usually slight, and the stage is therefore often called *easy glide*. Later, as other slip systems become activated, the intersection mechanism becomes predominant, resulting in much greater work-hardening. In a final stage, screw dislocations may come into play.

Since the number of possible mechanisms producing forces on dislocations is great, there is as yet no comprehensive theory of work-hardening that would permit the formulation of a stress-strain relation from dislocation theory. For reviews of work-hardening models, see Basinski and Basinski [1979] or Hirsch [1975].

Yield Strength of Polycrystals

The plastic deformation of polycrystals differs from that of single crystals in that, in the former, individual crystals have different orientations and therefore, under a given applied stress, the resolved shear stress varies from grain to grain. The critical value of this stress is therefore attained in the different grains at different values of the applied stress, so that the grains yield progressively. Furthermore, the grain boundaries present strong barriers to dislocation motion, and therefore the yield stress is in general a decreasing function of grain size, other factors being the same; the dependence is often found to be described by the **Hall–Petch relation**,

$$\sigma_Y = \sigma_{Y\infty} + \frac{k_Y}{\sqrt{d}},$$

where d is the grain diameter, and $\sigma_{Y\infty}$ and k_Y are temperature-dependent material constants.

The stress $\sigma_{Y\infty}$, corresponding (theoretically) to infinite grain size, may be interpreted as the yield stress when the effects of grain boundaries can be neglected. As such it should be determinable, in principle, from the single-crystal yield stress by a suitable averaging process, on the assumption of random orientation of the grains. Such a determination was made by Taylor [1938], who obtained the result that, if the stress-strain curve for a single crystal in shear on an active slip system is given by $\tau = f(\gamma^p)$, then for the polycrystal it is given by

$$\sigma = \bar{m} f(\bar{m} \varepsilon^p),$$

where \bar{m} is the average value of the factor $(\cos \phi \cos \lambda)^{-1}$ in Equation (2.2.1), a value that Taylor calculated to be about 3.1 for fcc metals.

Bauschinger Effect

A fairly simple explanation of the Bauschinger effect is due to Nabarro [1950]. The dislocations in a pile-up are in equilibrium under the applied

stress σ , the internal stress σ_i due to various obstacles, and the back stress σ_b due to the other dislocations in the pile-up; σ_i may be identified with the elastic limit. When the applied stress is reduced, the dislocations back off somewhat, with very little plastic deformation, in order to reduce the internal stress acting on them. They can do so until they are in positions in which the internal stress on them is $-\sigma_i$. When this occurs, they can move freely backward, resulting in reverse plastic flow when the applied stress has been reduced by $2\sigma_i$.

Exercises: Section 2.2

1. For a crystal with cubic symmetry, find the Young's modulus E in terms of C_{11} , C_{12} , and C_{44} for tension (a) parallel to a cube edge, (b) perpendicular to a cube edge and at 45° to the other two edges.
2. Show the close-packed planes and slip directions in a face-centered cubic crystals.
3. Derive Equation (2.2.1).
4. For what range of R/a do Equations (2.2.3) give Equation (2.2.4) with the values of α given in the text?

Section 2.3 Plasticity of Soils, Rocks, and Concrete

In recent years the term “geomaterials” has become current as one encompassing soils, rocks, and concrete. What these materials have in common, and in contrast to metals, is the great sensitivity of their mechanical behavior to pressure, resulting in very different strengths in tension and compression. Beyond this common trait, however, the differences between soils on the one hand and rocks and concrete on the other are striking. Soils can usually undergo very large shearing deformations, and thus can be regarded as plastic in the usual sense, although soil mechanicians usually label as “plastic” only cohesive, claylike soils that can be easily molded without crumbling. Rock and concrete, on the other hand, are brittle, except under high triaxial compression. Nevertheless, unlike classically brittle solids, which fracture shortly after the elastic limit is attained, concrete and many rocks can undergo inelastic deformations that may be significantly greater than the elastic strains, and their stress-strain curves superficially resemble those of plastic solids.

2.3.1 Plasticity of Soil

The Nature of Soil

The essential property of soils is that they are *particulate*, that is, they are composed of many small solid particles, ranging in size from less than 0.001 mm (in clays) to a few millimeters (in coarse sand and gravel). Permanent shearing deformation of a soil mass occurs when particles slide over one another. Beyond this defining feature, however, there are fundamental differences among various types of soils, differences that are strongly reflected in their mechanical behavior.

The voids between the particles are filled with air and water; the ratio of the void (air and water) volume to the solid volume is known as the *void ratio* of the soil. While much of the water may be in the usual liquid form (*free water*), and will evaporate on drying, some of the water is attached to the particle surfaces in the form of adsorbed layers, and does not evaporate unless the solid is heated to a temperature well above the boiling point of water. A soil is called *saturated* if all the voids are filled with water. If both water and air are present, the soil is called *partially saturated*, and if no free water is present, the soil is called *dry*.

Clay was mentioned at the beginning of this chapter as a prototype of a plastic material. Clays are fine-grained soils whose particles contain a significant proportion of minerals known as *clay minerals*. The chemistry of these minerals permits the formation of an adsorbed water film that is many times thicker than the grain size. This film permits the grains to move past one another, with no disintegration of the matrix, when stress is applied. It is this property that soil mechanicians label as plasticity. Claylike soils are also generally known as *cohesive soils*.

In cohesionless soils, such as gravels, sands, and silts, the movement of grains past one another is resisted by dry friction, resulting in shear stresses that depend strongly on the compression. Materials of this type are sometimes called *frictional materials*.

Soil Compressibility

If soil that is prevented from expanding laterally is loaded in compression between layers, at least one of which is permeable to water, an irreversible decrease in void ratio occurs, a result of the seepage of water from the voids. The process, known as *consolidation*, takes time, and sometimes goes on indefinitely, though at an ever-diminishing rate, much like creep. As a rule, though, something very near the ultimate compression is attained in a finite time which depends on the properties of the soil layer. A typical compression curve is shown in Figure 2.3.1(a). The figure shows both the virgin curve and the hysteresis loop resulting from decompression followed by recompression. A soil that has been decompressed is called *overconsolidated*. The curves

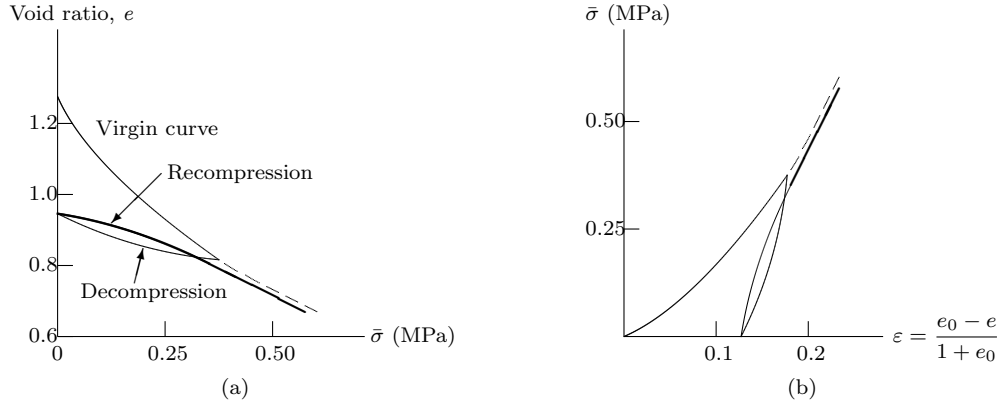


Figure 2.3.1. Compression curve for soil: (a) consolidation curve; (b) compressive stress-strain diagram [(b) is (a) replotted].

are replotted in Figure 2.3.1(b) as a compressive stress-strain diagram. It is seen that except for the upward convexity of the virgin curve, the diagram resembles that of work-hardening metals.

Shearing Behavior

As in ductile metals, failure in soils occurs primarily in shear. Unlike metals, the shear strength of soils is, in most circumstances, strongly influenced by the compressive normal stress acting on the shear plane and therefore by the hydrostatic pressure. Since soils have little or no tensile strength, the tension test cannot be applied to them. Other means are necessary in order to determine their shear strength.

Direct Shear Test. A traditional test of the shear strength of soft clays and of dry sands and gravels is the *direct shear test* or *shear-box test*. A sample of soil is placed in a rectangular box whose top half can slide over the bottom half and whose lid can move vertically, as shown in Figure 2.3.2(a). A normal load is applied to the lid, and a shear force is applied to the top half of the box, shearing the soil sample.

Simple Shear Test. In this test, developed by Roscoe [1953], it is the strain that is maintained as one of simple shear [see Figure 2.3.2(b)].

The two tests just described, along with others like them, provide simple means of estimating the shear strength. However, the stress distribution in the sample is far from uniform, so that these tests do not actually measure stress, and no stress-strain diagrams can result from them.

Triaxial Test. This is generally regarded as the most reliable test of the shearing behavior of soils. As we shall see, it is used to test rock and concrete as well. This test was discussed in 2.2.1; a normal compressive stress σ_3 ($= \sigma_2$) is applied to the sides of a cylindrical sample by means of air or

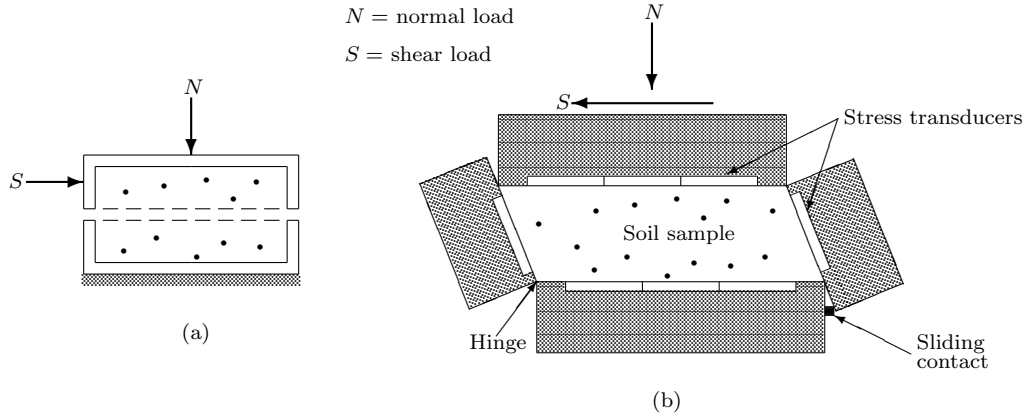


Figure 2.3.2. Shear tests: (a) direct shear test; (b) simple shear test (after Roscoe [1953]).

water pressure, and an axial compressive stress σ_1 , numerically greater than σ_3 , is applied at the ends (Figure 2.3.3). The results are commonly plotted

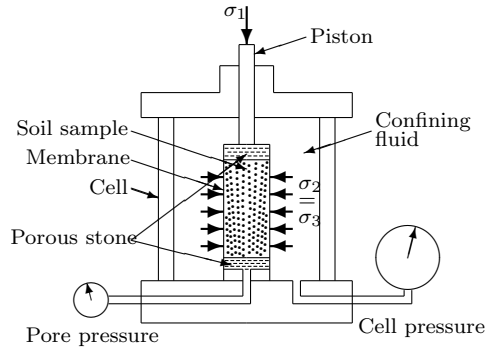


Figure 2.3.3. Triaxial test apparatus.

as graphs of $\sigma_1 - \sigma_3$ against the axial shortening strain ϵ_1 , with σ_3 as a parameter. (Alternatively, the mean stress $(\sigma_1 + 2\sigma_3)/3$ or the normal stress on the maximum-shear plane $(\sigma_1 + \sigma_3)/2$ may be used as a parameter.) Note that $\sigma_1 - \sigma_3$ is a measure both of the maximum shear stress given by Equation (1.3.11), namely, $\tau_{\max} = \frac{1}{2}|\sigma_1 - \sigma_3|$, and of the octahedral shear stress, given in accordance with Equation (1.3.5) as $\tau_{\text{oct}} = (\sqrt{2}/3)|\sigma_1 - \sigma_3|$. If $\sigma_3 = 0$ then the test is called an *unconfined compression test*, used most commonly on hard materials such as rock and concrete, but occasionally on clay if it is performed fast enough (“quick test”). Some typical stress-strain curves for soils are shown in Figure 2.1.1(f) (page 78).

The dependence of the shear strength of soils on the normal stress acting on the shearing plane varies with the type and condition of the soil. It is sim-

plest in dry cohesionless soils (gravels, sands, and silts), in which resistance to shear is essentially due to dry friction between the grains, and therefore is governed by the Coulomb law of friction:

$$\tau = \sigma \tan \phi, \quad (2.3.1)$$

where τ and σ are respectively the shear and normal stresses on the shearing plane, and ϕ is the *angle of internal friction*, a material property.

In wet cohesionless soils, the applied stress is the sum of the *effective stress* in the grains and the *neutral stress* due to water pressure and possibly capillary tension. If the latter stress is denoted σ_w (like σ , positive in compression), then the Coulomb law is expressed by

$$\tau = (\sigma - \sigma_w) \tan \phi, \quad (2.3.2)$$

since the water pressure provides a counterthrust on potential sliding surfaces, and therefore it is only the effective stress that governs frictional resistance. The concept of effective stress is due to Terzaghi.

Cohesionless soils also undergo significant volume changes when sheared. They tend to swell if they are dense, since closely packed grains must climb over one another in the course of shearing, and shrink if they are loose, since grains fall into the initially large voids and thus reduce the void volume. A granular soil thus has a *critical density* which remains essentially constant as shearing proceeds, and the soil is termed *dense* or *loose*, respectively, if its density is above or below critical.

In a sample of fine sand or silt that is dense and saturated, and which has no source of additional water, the swelling that accompanies shearing produces surface tension on the water which acts as a negative neutral stress. Consequently, in accord with Equation (2.3.2), such a sample has shear strength under zero applied stress.

In clays, the stresses in the adsorbed water layers play an important role in determining strength, and in partially saturated clays this role is predominant. The shear strength of such clays is given approximately by

$$\tau = c + \sigma \tan \phi, \quad (2.3.3)$$

where ϕ is the angle of internal friction and c is a material constant called the *cohesion*, representing the shear strength under zero normal stress.

The shear response of a saturated clay depends on whether it is in a *drained* or *undrained* condition. The former condition is achieved in a slow application of the stresses, so that the neutral stresses are not changed during the loading and therefore play little part in determining the shear strength. Equation (2.3.1) is consequently a good approximation to the relation between shear stress and normal stress in this condition. In the undrained

condition, on the other hand, the loading is quick and the applied stress is carried by the neutral stress. In this condition the shear strength is independent of the applied normal stress, and is therefore given by Equation (2.3.3) with $\phi = 0$; the cohesion c is then called the *undrained strength* and denoted c_u . Volume changes accompanying shearing are negligible in saturated clays. The shear-strength response of undrained clays thus resembles that of metals. Much of soil engineering practice is based on this model, though it is not universally accepted; see Bolton [1979], Section 5.1, for a survey of the criticisms.

2.3.2 “Plasticity” of Rock and Concrete

Unlike soils, materials such as rock, mortar and concrete are generally not plastic in the sense of being capable of considerable deformation before failure. Instead, in most tests they fracture through crack propagation when fairly small strains (on the order of 1% or less) are attained, and must therefore be regarded as brittle. However, concrete, mortar, and many rocks (such as marble and sandstone) are also unlike such characteristically brittle solids as glass and cast iron, which fracture shortly after the elastic limit is attained. Instead, they attain their ultimate strength after developing permanent strains that, while small in absolute terms, are significantly greater than the elastic strains. The permanent deformation is due to several mechanisms, the foremost of which is the opening and closing of cracks.

Strain-Softening

Following the attainment of the ultimate strength, concrete and many rocks exhibit *strain-softening*, that is, a gradual decrease in strength with additional deformation. The nature of this decrease, however, depends on factors associated with the testing procedure, including sample dimensions and the stiffness of the testing machine.

The effect of machine stiffness can be described as follows. Let P denote the load applied by the machine to the sample, and u the sample displacement. In the course of a small change Δu in the displacement, the sample absorbs energy in the amount $P\Delta u$. If the machine acts like an elastic spring with stiffness k , then a change ΔP in the load implies a change $P\Delta P/k$ in the energy stored in the machine. This change represents *release* of energy if $P\Delta P < 0$, that is, once softening takes place. The energy released by the machine is greater than that which can be absorbed by the sample if $k < |\Delta P/\Delta u|$, resulting in an unstable machine-sample system in the case of a “soft” machine; the sample breaks violently shortly after the ultimate strength is passed. A “stiff” machine, on the other hand, makes for a system that is stable under displacement control. It is only with a stiff machine, therefore, that a complete load-displacement (or stress-displacement) curve

can be traced.

It is not certain, however, whether the stress-displacement curve may legitimately be converted into a stress-strain curve, such as is shown in Figure 2.1.1(d) (page 78), that reflects material properties, since specimen deformation is often far from homogeneous. Experiments by Hudson, Brown and Fairhurst [1971] show a considerable effect of both the size and the shape of the specimens on the compressive stress-strain curve of marble, including as a particular result the virtual disappearance of strain-softening in squat specimens. Read and Hegemier [1984] conclude that no strain-softening occurs in specimens of soil, rock and concrete that are homogeneously deformed. A similar conclusion was reached by Kotsovos and Cheong [1984] for concrete. It should be remarked that some rocks, such as limestone, exhibit classically brittle behavior in unconfined compression tests even with stiff testing machines — that is, they fracture shortly after the elastic limit is reached.

The Effect of Pressure

An important feature of the triaxial behavior of concrete, mortar and rocks (including those which are classically brittle in unconfined tests) is that, if the confining pressure σ_3 is sufficiently great, then crack propagation is prevented, so that brittle behavior disappears altogether and is replaced by ductility with work-hardening. Extensive tests were performed on marble and limestone by von Kármán [1911] and by Griggs [1936]; some results are shown in Figure 2.1.1(e). Note that the strains attained in these tests can become quite large.

The relation between hydrostatic pressure and volumetric strain also exhibits ductility with work-hardening; the curves resemble those of Figure 2.3.1(b). It can be said, in general, that rocks and concrete behave in a ductile manner if all three principal stresses are compressive and close to one another.

Dilatancy

If the transverse strain $\varepsilon_2 = \varepsilon_3$ is measured in uniaxial compression tests of rock and concrete specimens in addition to the axial strain ε_1 , then, as discussed in 1.2.2, the volumetric strain ε_V equals $\varepsilon_1 + \varepsilon_2 + \varepsilon_3$. If the stress σ_1 is plotted against ε_V (positive in compression), it is found that ε_V begins to decrease from its elastic value at stresses greater than about half the ultimate strength, reaches zero at a stress near the ultimate strength, and becomes negative (signifying an *increase* in volume) in the strain-softening range (see Figure 2.3.4, showing both a σ_1 - ε_1 and a σ_1 - ε_V diagram). Similar results are obtained in triaxial tests under low confining pressures. This volume increase, which results from the formation and growth of cracks parallel to the direction of the greatest compressive stress, is known as *dilatancy*. This term is sometimes also applied to the swelling of dense granular soils,

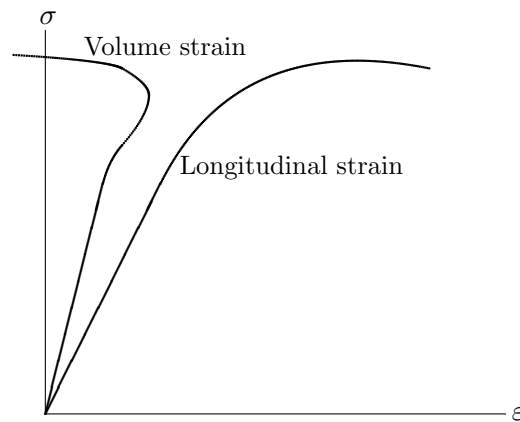


Figure 2.3.4. Compression tests on concrete or rock: stress against longitudinal strain and volume strain.

although the mechanism causing it is unrelated.

Tensile Behavior

Uniaxial tension tests are difficult to perform on rock and concrete, and the results of such tests vary considerably. The most reliable direct tension tests are those in which the ends of the specimen are cemented with epoxy resin to steel plates having the same cross-section as the specimen, with the tensile force applied through cables in order to minimize bending effects. The uniaxial tensile strength of rock and concrete is typically between 6 and 12% the uniaxial compressive strength. Strain-softening, associated with the opening of cracks perpendicular to the direction of tension, is observed in tests performed in stiff machines.